

AJTE99-6429

## NUMERICAL SIMULATION OF POOL BOILING FOR STEADY STATE AND TRANSIENT HEATING

Ying He, Masahiro Shoji and Shigeo Maruyama

Department of Mechanical Engineering, Faculty of Engineering,  
The University of Tokyo, Tokyo, Japan  
E-mail: ying@photon.t.u-tokyo.ac.jp

*Keywords:* Macrolayer, Vapor stem, Numerical Simulation, Pool boiling, Transient boiling

### ABSTRACT

It's believed that the macrolayer plays an important role in nucleate and transition boiling heat transfer at high heat flux. Many experiments have been carried out to support the macrolayer evaporation model, however, little has been conducted in the numerical simulation of boiling heat transfer. In this study, based on the macrolayer evaporation model of Maruyama et al. (1992), a numerical simulation of pool boiling for steady state was carried out. The key points of the simulation are: (1) It is modeled that the macrolayer containing vapor stems occupies the region immediately next to the wall and that the vapor stems are formed on the active cavity sites. (2) Not only does the evaporation occur at the vapor bubble-macrolayer interface, but also at the liquid-vapor stem interface. (3) The macrolayers form periodically. No liquid is supplied to the macrolayers during the hovering period. While the vapor mass departs from the surface, the macrolayers replenish immediately despite of the complicity of the transition period between the departures of two vapor masses. The major results are: (1) The boiling curves of water and FC-72 ( $C_6F_{14}$ ) were reasonably predicted. (2) The temporal variations in surface temperature for different boiling regimes were obtained.

Secondly, the simulation of transient pool boiling was conducted. It was realized with following assumptions:

- (1) The macrolayer evaporation model can be extended to the transient pool boiling. The macrolayer forms cyclically and its thickness is determined by the surface heat flux when the vapor mass takes off.
- (2) One-dimensional transient heat conduction within the heater coupled with the macrolayer model was considered. Being employed explicit FDM, the instantaneous surface

temperature can be obtained. Therefore, the instantaneous heat flux can be calculated by applying the surface temperature into the macrolayer model.

(3) In the transition-boiling regime, the initial thickness of macrolayer was determined by the extrapolated value of the obtained nucleate boiling curve.

The simulated results showed that:

(a) For lower transient heating rate, the boiling curve in the nucleate boiling regime almost remains the same as the steady-state curve. For higher transient heating rate, it deviates from the steady-state curve.

(b) The critical heat flux increases with increasing heating transients. The investigation of the changes of macrolayer thickness and void fraction implies that the evaporation of macrolayer has a great effect on the increase of CHF under transient heating.

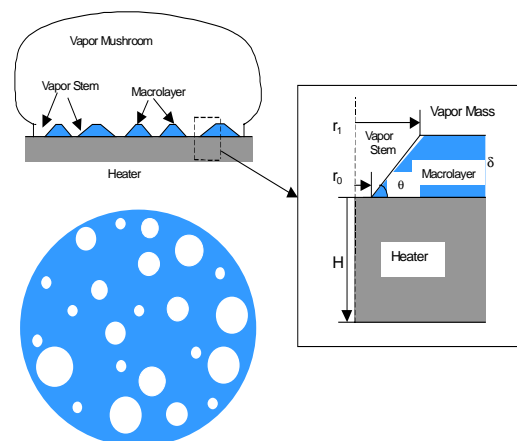


Figure A-1 Schematics of Macrolayer Model

## NOMENCLATURE

A = area, m<sup>2</sup>  
g = gravitational acceleration, m/s<sup>2</sup>  
H<sub>fg</sub> = latent heat of evaporation, J/kg  
N = number of molecules per volume  
q = instantaneous heat flux, W/m<sup>2</sup>  
q<sub>av</sub> = time averaged heat flux, W/m<sup>2</sup>  
q<sub>m</sub> = Gambill-Lienhard upper limit heat flux, W/m<sup>2</sup>  
Q = heat transfer rate, W  
r<sub>s</sub> = radius of a vapor stem, m  
r = radial coordinate from the center of a vapor stem, m  
R = ideal gas constant, J/kgK  
T<sub>w</sub> = surface temperature, °C  
t = time, s  
v = mean velocity of molecules, m/s  
α<sub>1</sub> = void fraction  
α = thermal diffusivity, m<sup>2</sup>/s  
δ = macrolayer thickness, m  
δ<sub>m</sub> = macrolayer thickness corresponded to q<sub>m</sub>, m  
λ = thermal conductivity, W/mK  
θ = contact angle  
ρ<sub>molec</sub> = mass of a molecule  
ρ<sub>l</sub> = density of liquid, kg/m<sup>3</sup>  
ρ<sub>v</sub> = density of vapor, kg/m<sup>3</sup>  
σ = surface tension, N/m  
τ = bubble departure period, s

## Subscripts

h = heater  
l = liquid  
v = vapor  
w = heated surface

## INTRODUCTION

Understanding the mechanism of boiling heat transfer during steady state and transient condition is very important in steel industry and nuclear reactor technology. For the steady-state pool boiling, a number of models have been proposed. Among them, there are several modeling efforts that focus on the instabilities in the tiny vapor passages that are postulated to intersperse the liquid-rich macrolayer immediately adjacent to the heater surface.

Haramura & Katto(1983) and Pan et al. (1989) suggested an alternate CHF theory basing on the role of the macrolayer. These models retained the basic element of Zuber (1959)'s model that hydrodynamic instabilities dictate the occurrence of CHF. However, they proposed that the controlling instabilities occur not at the walls of large vapor columns but rather at the walls of tiny vapor stems around active nucleate cavities that intersperse the liquid macrolayer on the heater surface itself.

Another representative model was reported by Dhir &

Liaw (1989). They deduced an area and time-averaged model from experimental measurements of void fraction close to the heater surface. In the model, the energy from the wall is conducted into liquid macro/micro layer surrounding the stems and is utilized in evaporation at the stationary liquid-vapor interface. They proposed that the heat flux be predicted as

$$q_w = h_l(1 - \alpha_w)\Delta T_{ws} + h_v\alpha_w\Delta T_{ws} \quad (1)$$

where α<sub>w</sub> is the void fraction at the wall. The heat transfer coefficient in the dry region was taken to be that given by a correlation for film boiling. The heat transfer coefficient in the wet region was obtained by solving two-dimensional conduction equation for the liquid-occupied region. The analysis is based on the assumption that all dissipation of liquid occurs on the walls of the vapor stems.

Although the two models can explain critical heat flux and transition boiling fairly well, there appears to be some discrepancies with each other.

Maruyama et al. (1992) presented a model basing on the macrolayer theory. The model retains the basic thought of Haramura & Katto's model (1983) that the macrolayer forms underneath the coalesced bubble and dries out periodically. The difference is about the assumption of vapor stems. The model developed by Maruyama et al. (1992) postulated that vapor stems are formed on the active cavity sites with a certain contact angle and the evaporation also occurs at the liquid-vapor interface. However, Haramura & Katto (1983) assumed that the liquid-vapor interface was stationary and the entire surface heat flux contributes to macrolayer evaporation. Therefore, only the height of vapor stems decreases with time. In fact, this model can be considered to be the combination of the spatial-averaged and time-averaged model.

With respect to transient boiling processes, a large number of experimental studies have been conducted. Sakurai and Shiotsu (1977a, 1977b) obtained transient boiling data using a platinum wire of 1.2mm in diameter in a pool of saturated water by increasing input power exponentially. The heat generation rate per unit volume is expressed as

$$Q(t) = Q_i \exp\left(\frac{t}{t_0}\right) \quad (2)$$

The exponential period of heat generation rate was varied from 5ms to 10s. The pressure changed from atmospheric to 2MPa. They concluded that the transient boiling could be divided into regular and irregular boiling. For the regular boiling, transient CHF is in the extension of the steady-state curve. In irregular boiling, the transient curve doesn't recover the steady-state curve and transient CHF become much higher.

Recently, Hohl et al. (1996) performed pool boiling experiments with controlled wall temperature transient. They obtained transient boiling data using a cylindrical copper block of 10-mm thickness and 34mm in diameter in a pool of saturated liquid FC-72. The experiment revealed that the characteristics of the transient boiling curve increases with wall temperature heating rates and decreases with cooling rates.

Pasamehmetoglu et al. (1990) and Zhao et al. (1997) reported the theoretical treatments of this problem. Pasamehmetoglu et al. (1990) provided a model for predicting transient CHF in saturated pool boiling. The developed model includes the analysis of heat conduction within the heater coupled with a macrolayer-thinning model. The prediction indicated favorable agreement with the experimental data except the fast transient when the exponential period of heat generation rate  $\tau_m$  is less than 20ms. However, the prediction was just compared to that of the heater of small diameter wires. In fact, the analytical model is based on the assumption that for the critical heat flux, the vapor bubble departs only when the macrolayer is dried out completely. This is inconsistent with the experiment by Kirby & Westwater (1965). Zhao et al. (1997) recently put forward a model for transient pool boiling heat transfer basing on their microlayer model. In their model, the evaporation of the microlayer below the individual bubbles was considered to play an important role in the nucleate boiling heat transfer. For the transient heating, they assumed that the population of individual bubbles increases with time and in each time-step a new group of bubbles with the same size form and grow up. Although the prediction showed the same tendency with the experimental data, it employed too high heating rate to be realized in practical experiments for a horizontal surface.

In this paper, basing on the model of Maruyama et al. (1992), we adopted theoretical method to determine macrolayer thickness and employed simple numerical method to obtain the boiling curve of water and FC-72 for the steady-state condition. In addition, the model was developed to apply in the transient boiling process. The transient boiling curves were predicted through increasing power linearly and exponentially. The results showed a favorable agreement with the experiment of Hohl et al. (1996) and the same tendency with the experiment of Sakurai et al. (1977).

## NUMERICAL SIMULATION FOR STEADY STATE

### Governing Equations

Figure 1 shows the schematic of the top and side views of a vapor bubble on a heated surface. In this model, the macrolayer containing vapor stems occupies the region immediately next to the wall. The vapor stems are formed on the active cavity sites. The most important feature of this model is the introduction of a liquid-vapor stem interface

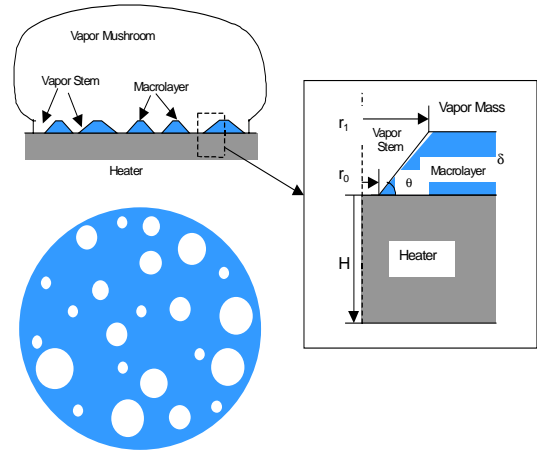


**Figure 1. Model of heat conduction and evaporation near the liquid-vapor interface**

evaporation phenomenon, which means that not only does the evaporation occur at the vapor bubble-macrolayer interface but also at the stem interface.

In this part of the simulation, we assumed the wall temperature was uniform and constant. The influence of temperature variation in the heater was not considered. From the heater surface heat is conducted into the macrolayer and is utilized in evaporation at the macrolayer-bubble interface. Therefore, the heat balance is written as

$$-\rho_l H_{fg} \frac{d\delta}{dt} = \frac{\lambda \Delta T}{\delta} \quad (3)$$

By the integration of equation (3), the thickness of macrolayer can be obtained as

$$\delta(t) = \sqrt{\delta_0^2 - 2 \frac{\lambda \Delta T}{\rho_l H_{fg}} t} \quad (4)$$

where  $\lambda$  is heat conductivity of liquid,  $\rho_l$  is density of liquid,  $H_{fg}$  is latent heat of evaporation,  $\Delta T$  is wall superheat, and  $\delta_0$  is the initial thickness of macrolayer.

The rate of heat transfer from the liquid-vapor stem interface can be written as

$$\begin{aligned} Q &= \int q dA = \int_{r_0}^{r_1} q 2\pi r dr \\ &= 2\pi r_0 \lambda \Delta T \frac{1}{\tan \theta} \left[ 1 + \left( \frac{\delta}{r_0 \tan \theta} \right) + \log \left( \frac{\delta}{\delta_m} \right) \right] \end{aligned} \quad (5)$$

Where A is the liquid-vapor stem interface area. Suppose that heat from the heated surface is conducted into the interface area and is applied in the evaporation at the stem-liquid

interface. The evaporated heat just contributes to the increase of radius of the vapor stem. Therefore, the heat balance can be written as

$$\int q dA = \rho_l H_{fg} A \frac{dr_s}{dt} \sin \theta \quad (6)$$

where  $\theta$  is defined as the contact angle according to the model. The growth rate of vapor stems  $dr_s/dt$  is then obtained from equations (5) and (6) as

$$\frac{dr_s}{dt} = \frac{1}{\rho_l H_{fg}} \frac{\lambda \Delta T}{\delta} \frac{1}{\tan \theta} \times \left[ \frac{1 + \left( \frac{\delta}{r_0 \tan \theta} \right) + \log \left( \frac{\delta}{\delta_m} \right)}{\left( 1 + \left( \frac{\delta}{2r_0 \tan \theta} \right) \right)} \right] \quad (7)$$

Because  $\delta/(r_0 \tan \theta) \ll 1$ , thus equation (7) can be simplified as

$$\frac{dr_s}{dt} = \frac{1}{\rho_l H_{fg}} \frac{\lambda \Delta T}{\delta} \left[ 1 + \log \left( \frac{\delta}{\delta_m} \right) \right] \quad (8)$$

where  $\delta_m$  is the thickness corresponding to the maximum evaporation heat flux for saturated pool boiling. The introduction of  $\delta_m$  to avoid the infinite heat flux at the liquid-vapor interface. The maximum evaporation heat flux can be obtained by considering the evaporation and condensation of molecules. There exists vapor pressure difference when the surface is at the superheated condition. The mass velocity of evaporated molecules is expressed as

$$\Delta m = \rho_{molec} N v = \rho_v v = \frac{\Delta p}{\sqrt{2\pi R T_{sat}}} \quad (9)$$

By Clausius-Clapeyron equation, the relation between pressure difference and superheat can be written as

$$\frac{\Delta p}{\Delta T} = \frac{H_{fg}}{T_{sat} \left( \frac{1}{\rho_v} - \frac{1}{\rho_l} \right)} \quad (10)$$

The upper limit heat flux thus can be written as

$$q_m = \Delta m H_{fg} = \frac{\rho_l}{\rho_l - \rho_v} \frac{\rho_v H_{fg}}{T_{sat}} \frac{H_{fg}}{\sqrt{2\pi R T_{sat}}} \Delta T \quad (11)$$

For saturated pool boiling of water at atmospheric pressure, the upper limit heat flux can be expressed as

$$q_m = 7.86 \Delta T (MW / m^2) \quad (12)$$

Therefore,  $\delta_m$  can be expressed from equation (3) as

$$\delta_m = \frac{\lambda \Delta T}{q_m} \quad (13)$$

In order to calculate the instantaneous heat flux  $q$ , we introduce a parameter  $w$ , which is defined as the equivalent thickness. It means the amount of liquid left on the surface. It can be expressed as  $w = \delta(1 - \alpha_l)$ . The instantaneous heat flux can be written as

$$\begin{aligned} q &= \rho_l H_{fg} \left( -\frac{dw}{dt} \right) \\ &= \rho_l H_{fg} (1 - \alpha_l) \left( -\frac{d\delta}{dt} \right) + \rho_l H_{fg} \delta \frac{d\alpha_l}{dt} \\ &= q_{\alpha_l} + q_{\delta} \end{aligned} \quad (14)$$

where  $q_{\alpha_l}$  and  $q_{\delta}$  are heat fluxes related to the decay of macro-layer thickness and the growth of vapor stems, respectively.

The macrolayer theory considers that the liquid supply occurs periodically and the departure period exactly corresponds to the sustained period of vapor bubble. Therefore, the averaged heat flux can be expressed as

$$q_{av} = \frac{1}{\tau} \int_0^{\tau} q dt \quad (15)$$

### Vapor Stems, Initial Macrolayer Thickness and Bubble Departure Period

With respect to the initial void fraction, Gaertner (1965) showed that the diameter of the vapor stems had the relationship with the active site population for water as

$$D^2 \frac{N}{A} = \frac{1}{9} \quad (16)$$

Where  $D$  is the diameter of the vapor stem,  $N/A$  is the active site population. In this simulation, the diameters of the vapor stems were controlled within 0.4mm according to the experiments. On the basis of the above equation, the active site population was between  $1.15 \times 10^6 \sim 1.53 \times 10^6 m^{-2}$ .

Rajavanshi et al. (1992) put forward an equation about initial macrolayer thickness according to Haramura & Katto's

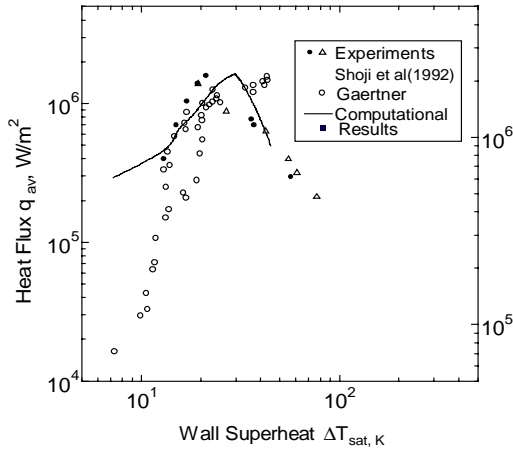


**Figure 2. Comparison of the model prediction with the experimental data**

hypothesis (1983), i.e.

$$\delta_0 = 0.0107\sigma\rho_v \left(1 + \frac{\rho_v}{\rho_l} \left(\frac{\rho_v}{\rho_l}\right)^{0.4} \left(\frac{H_{fg}}{q_{av}}\right)^2\right) \quad (17)$$

In this simulation, for a given heat flux, the initial macrolayer thickness was obtained by equation (17). In the transition boiling regime, the extrapolated values of the equation were employed as the initial macrolayer thickness. The bubble departure period is according to the equation of Katto & Yokoya(1975), i.e.

$$\tau = \left(\frac{3}{4\pi}\right)^{\frac{1}{5}} \left[\frac{4(\xi\rho_l + \rho_v)}{g(\rho_l - \rho_v)}\right]^{\frac{3}{5}} v_1^{\frac{1}{5}} \quad (18)$$

### Results for Steady State

Because the heat flux is the function of wall superheat, from nucleate boiling regime to the critical heat flux, we can obtain the numerical solution of wall superheat by the bisection method. To be specific, initially, for a given heat flux, we obtained the initial macrolayer thickness by equation (17). Subsequently, we calculated the heat flux in a certain wall superheat by using the above macrolayer model. Finally, If the difference between the calculated and the given heat flux was less than a decided convergence coefficient, the wall superheat could be considered the numerical solution of the given heat flux. In the transition boiling regime, we employed the wall superheat as the given condition instead, the initial macrolayer thickness was gained through the extrapolated line of the boiling curve in nucleate boiling regime. Therefore, the heat flux can be calculated by the present model.

Figure 2 shows the simulated boiling curve. The diameter of simulated area was 10mm. As shown, the prediction in the high heat flux regime is in a good agreement

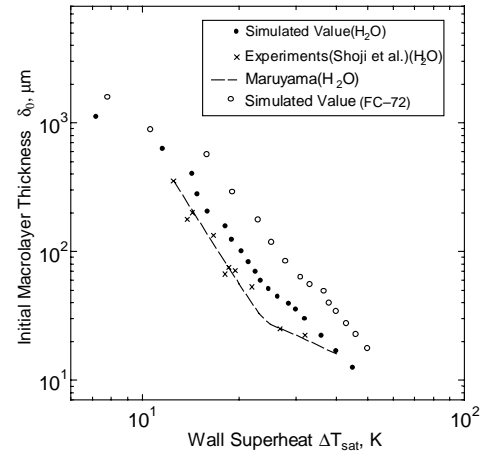


**Figure 3. Simulated Initial Macrolayer Thickness**

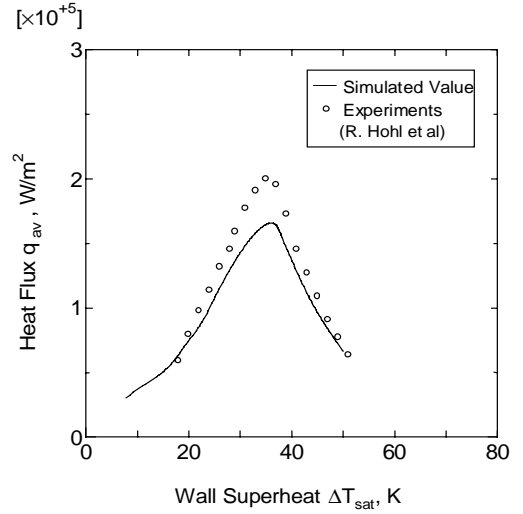


**Figure 4. Simulated boiling curve of FC-72**

with the experiments, however, it predicted higher in the low heat flux regime. This implies that this model is more suitable for the high heat flux regime.

The relationship between the initial macrolayer thickness and wall superheat is shown in Figure 3. It can be seen that the change of initial macrolayer thickness is closely related to the change of heat flux. Different decreasing rates corresponds to the different boiling regime. Near the critical heat flux condition, the decreasing rate changes considerably, therefore, different boiling regimes appear.

The boiling curve of FC-72 was also calculated. The fluid was saturated at a temperature of 329K. The averaged bubble departure period of FC-72 was calculated as 30ms from equation (18). The results are plotted in Figure 4. We can see that except the lower critical heat flux, they are almost consistent with the experimental values carried out by Hohl et al. (1997). The predicted critical heat flux by the present model is  $q = 1.7 \times 10^5 \text{ W/m}^2$  at  $\Delta T = 36 \text{ K}$ . The lower heat flux

than the experimental value may be due to the smaller simulated area of the heater.

### SIMULATION OF TRANSIENT BOILING

The macrolayer evaporation model was extended to the transient boiling. Some assumptions were included as follows:

(1) The macrolayer form periodically. While the vapor mass departed from the surface, the macrolayer established immediately without a transition period before the formation of the new vapor mass. The initial thickness of the macrolayer is determined by the surface heat flux when the vapor mass takes off.

(2) The initial void fraction is not changed with wall temperature. This is consistent with Gaertner (1965)'s deduction that the product of the diameter of the vapor stems and the active site population remains the same, although the active site population increases with the wall superheat.

The motion pictures of Katto and Yokoya(1970) show that the liquid supply is initiated before the formation of vapor mass, however, the delay time of the new vapor bubble is much smaller than the bubble hovering period. Therefore, it is reasonable to make the assumption (1).

Besides the evaporation of macrolayer at heated surface, one-dimensional transient heat conduction within the heater was also considered. The heat conduction equation is

$$\frac{\partial T}{\partial t} = \alpha \frac{\partial^2 T}{\partial x^2} \quad (19)$$

Subjecting to the following initial and boundary conditions:

$$t = 0, \quad q_k = q_{in0}, \quad T_w = T_0 \quad (20)$$

$$x = 0, \quad -\lambda \frac{\partial T}{\partial x} = q_k \quad (21)$$

$$x = H, \quad -\lambda \frac{\partial T}{\partial x} = q_{in} \quad (22)$$

Where  $T_0$  is the initial averaged wall temperature,  $q_k$  is the instantaneous heat flux of boiling heat transfer, and  $q_{in}$  is the input heat flux from the bottom of the heater. Employing explicit FDM, we can obtain the instantaneous surface temperature and the instantaneous heat flux can be calculated by applying surface temperature into the macrolayer model.

### Results for Transient Heating

The input heat flux was set to increase linearly and exponentially. The incipient boiling superheats of water and FC-72 were set at 10K and 15K respectively. The simulated area is 10mm in diameter and the heater is copper with 10mm in thickness. The bubble departure periods of water and FC-72 are calculated by equation (18). Because the bubble

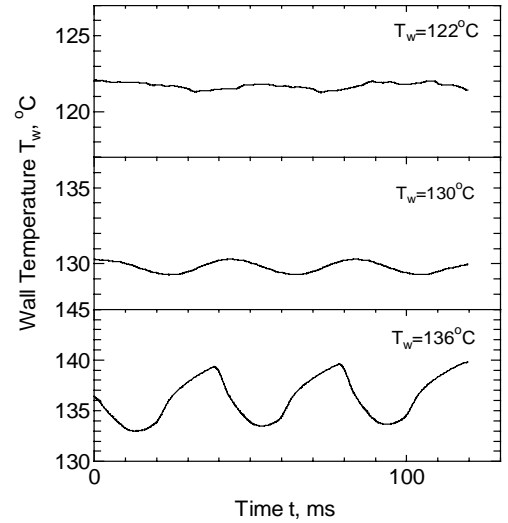


Figure 5. Temporal variations of wall temperature predicted for Steady State

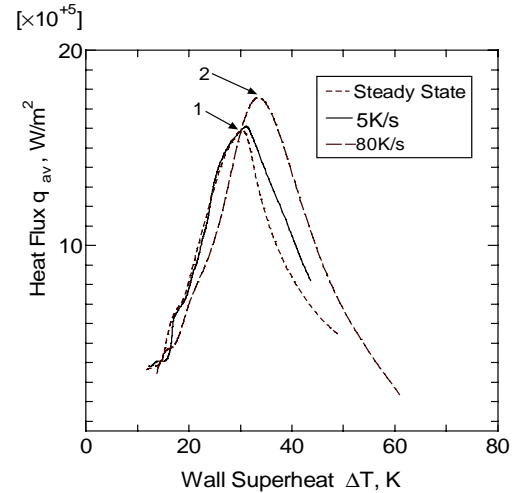
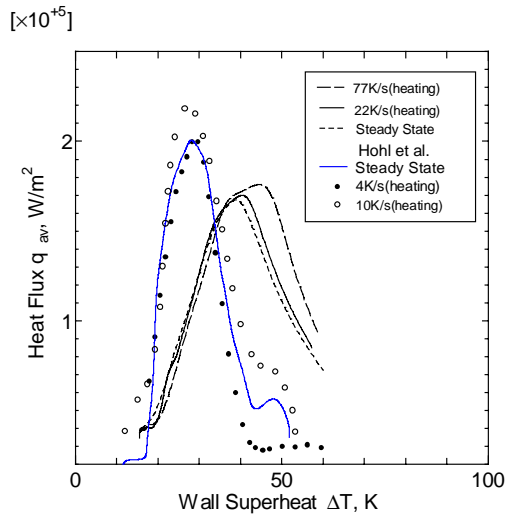


Figure 6. Predicted transient boiling curves of water

departure periods didn't change so much according to Huang(1993), we employed the averaged values as 40ms and 30ms respectively. The averaged heat flux increases with time and reaches the peak value automatically. We first investigated the wall temperature variation when the heating rate is zero, which is namely at steady state. The result is plotted in Figure 5. In nucleate boiling regime ( $T_w=122^\circ\text{C}$ ), the variation is very small. With the wall superheat increasing, the fluctuation becomes larger, especially in transition boiling regime. This is because the macrolayer is considerably thin and is consumed completely within a short period.

The boiling curves of water and FC-72 are plotted in Figure 6 and Figure 7. From these two figures, we can see that the boiling curves change with the heating rates. For lower transients, boiling curves almost remain the same as the



**Figure 7. Simulated transient boiling curves of FC-72 for different heating rates**

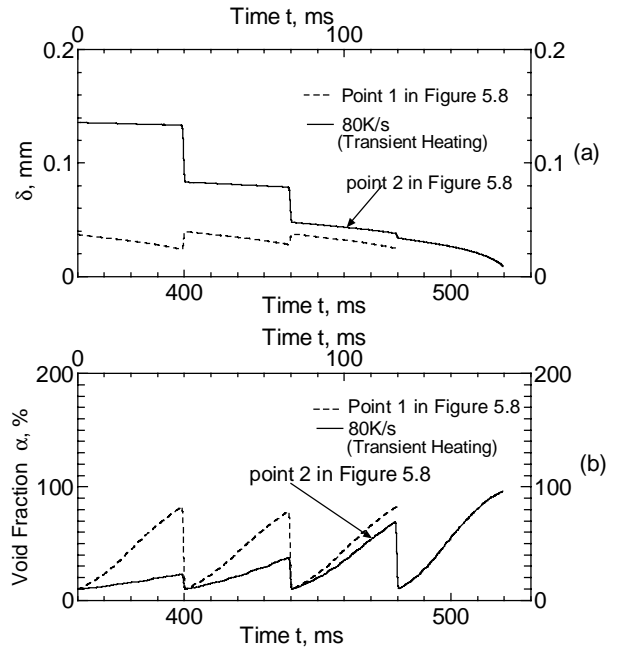


**Figure 9. Comparison of characteristic parameters for transient boiling and steady state (a) changes of macrolayer thickness (b) changes of void fraction**

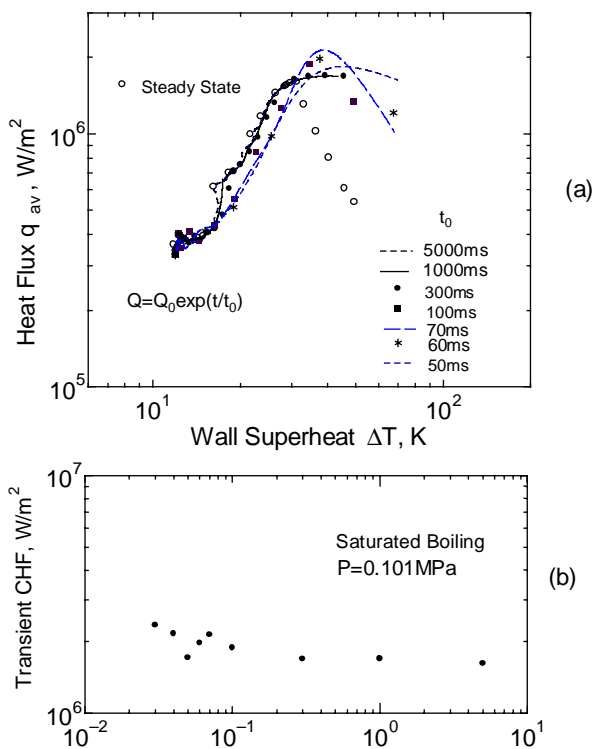


**Figure 8. Predicted results by exponential Heating increase (a) transient boiling curves (b) relationship between transient CHF and exponential period**

steady-state curve. Beyond the steady-state CHF, the nucleate boiling curves extend until the transient CHF is reached. For higher transient heating rate, the boiling curves deviate from the steady-state curve and the CHF becomes much higher. The experimental data by Hohl et al. (1996) are also plotted in

Figure 7. It's found that the simulated results have the same tendency as the experimental data. In Hohl et al. (1996)'s experiment, the diameter of heater was 34mm, this may be the reason that the CHF values are higher than the simulated results.

The transient boiling curves of water with increasing heat input exponentially are plotted in Figure 8(a). The exponential periods are varied from 5s~50ms. It shows the same characteristics as that shown in Figure 6. The change of transient CHF with time is plotted in Fig. 8(b). It can be seen that transient CHF generally increases the increase of heating rate. This tendency is the same as Sakurai et al. (1977, Part 2)'s experiment on a thin wire. However, the transient CHF begins to fluctuate when  $t_0$  is less than 70ms. The reason may be because the formation of macrolayer becomes unsteady.

We also tried to analyze the mechanism that the transient boiling curves change with heating rates. Figure 9(a) shows the changes of macrolayer thickness, and Figure 9(b) shows the changes of void fraction of point 1(steady state) and point 2(transient) in Figure 6. We can see that the macrolayer thickness of point 2 is thicker than that of point 1, whereas the instantaneous void fraction  $\alpha$  of point 2 is a little less than that in point 1. This may suggest that because of the thicker macrolayer thickness in transient boiling, the transient CHF becomes higher than the steady-state CHF.

## SUMMARY AND CONCLUSIONS

1. In this study, by using bisection method, the boiling curves of water and FC-72 were obtained. The results show that the macrolayer model is more suitable for the high heat flux regime

2. The macrolayer model was extended to transient boiling. Combining the original model and one-dimensional transient heat conduction within the heater, we obtained transient boiling curves of water and FC-72 by increasing input heat linearly and exponentially. The results are in an agreement with the experiment of Hohl et al. (1996).

3. By investigating the characteristic parameters for steady state and transient boiling, we found macrolayer thickness plays more important role on the transient boiling.

4. In this simulation, we assumed that the surface temperatures were uniform spatially. It has been known that spatial variations in surface temperature may not be overlooked. In the next step, we should simulate the temporal and spatial variations of wall temperature.

## REFERENCE

- Dhir, V. K., and Liaw, P., 1989, "Framework for Unified Model for Nucleate and Transition Pool Boiling," *Trans. ASME, J. Heat Transfer*, Vol. 111, No.3, pp.739-746.
- Gaetner, R. F., and Westwater, J. W., 1960, "Population of Active Sites in Nucleate Boiling Heat Transfer," *Chem. Eng. Prog. Symp.*, Ser. 56., pp. 39-48.
- Gaetner, R. F., 1965, "Photographic Study of Nucleate Pool Boiling on a Horizontal Surface," *ASME, J. Heat Transfer*, Vol. 87, pp.17-29.
- Haramura, Y., and Katto, Y., 1983, "A New Hydrodynamic Model of Critical hat Flux, Applicable Widely to Both Pool and Forced Convection Boiling on Submerged Bodies in Saturated Liquids," *Int. J. Heat Mass Transfer*, Vol. 26. No. 2, pp.389-399.
- Hohl, R., Auracher, H., Blum, J., and Marquardt, W., "Pool Boiling Heat Transfer Experiments with Controlled wall Temperature Transients," *Proc. of the 2nd European Thermal Science and 14th UIT National Heat Transfer Conference*, Vol. 3(1996), pp.1647-1652.
- Hohl, R., Auracher, H., and Blum, J., 1997, "Identification of Liquid-Vapor Fluctuations between Nucleate and Film Boiling in Natural Convection," *Convective Flow and Pool Boiling Conference, Section II: Pool Boiling*, Kloster Irsee.
- Huang, Z. L., 1993, "A Study of Steady Transition Boiling of Water," Ph. D thesis, Faculty of Engineering, The University of Tokyo.
- Katto, Y., Yokoya, S., and Yasunaka, M., 1970, "Mechanism of Boiling Crisis and Transition Boiling in Pool Boiling," *Proc. 4th Int. heat Transfer Conf.*, Paris, vol.5, pp. B3.2.
- Katto, Y., and Yokoya, S., 1975, "Behavior of A Vapor Mass in Saturated Nucleate and Transition pool Boiling," *Trans. JSME*, Vol. 41, pp.294-305.
- Kirby, D. B., and Westwater, J. W., 1965, "Bubble and Vapor Behavior on a Heated Horizontal Plate During Pool Boiling Near Burnout," *Chem. Engr. Prog. Symp.*, Ser. 61, No. 57.
- Maruyama, S., Shoji, M., and Shimizu, S., 1992, "A Numerical Simulation of Transition Boiling Heat Transfer," *Proceedings of the 2nd JSME-KSME Thermal Eng. Conf.* pp3-345-3-348.
- Pan, C., Hwang, J. Y., and Lin, T. L., 1989, "The Mechanism of Heat transfer in Transition Boiling," *Int. J. Heat Mass Transfer*, Vol.32, pp.1337-1349.
- Pasamehmetoglu, K. O., Chappidi, P.R., Unal C., and Nelson, R. A., 1993, "Saturated Pool Nucleate Boiling Mechanism at High Heat Fluxes," *Int J. Heat Mass Transfer*, Vol. 36, No. 15, pp.3859-3868.
- Pasamehmetoglu, K. O., Nelson, R. A., and Gunnerson, F. S., 1990, "Critical heat Flux Modeling in Pool Boiling for Steady-State and Power Transients", *J. Heat Transfer, Trans. ASME*, Vol. 112, pp. 1048-1057.
- Rajvanshi, A.K., Saini, J.S., and Prakash, R., 1992, "Investigation of Macrolayer Thickness in Nucleate Pool Boiling at High Heat Flux," *Int. J. Heat mass Transfer*, Vol.35, No. 2, pp. 343-350.
- Sadasivan, P., Unal, C. Nelson, R. A., 1995, "Perspective: Issues in CHF Modeling – The Need for New Experiments," *Trans. ASME, J. Heat Transfer*, Vol. 117, pp.558-567.
- Sakurai, A. and Shiotsu, M. 1977, "Transient Pool Boiling Heat Transfer, Part 1: Incipient Boiling Superheat," *ASME, J. Heat Transfer*, Vol. 99, pp.547-553.
- Sakurai, A. and Shiotsu, M. 1977, "Transient Pool Boiling Heat Transfer, Part 2: Boiling Heat Transfer and Burnout," *ASME, J. Heat Transfer*, Vol. 99, pp.554-560.
- Shoji, M., 1992, "Study of Steady Transition Boiling of Water: Experimental Verification of Macrolayer Evaporation Model," *Pro. Eng. Found. Conf. Pool External Flow Boiling*, Publ. by ASME, pp.237-242.
- Shoji, M., Kuroki, H., 1994, "Model of Macrolayer Formation in Pool Boiling," *Pro. of 10th Int. Heat Transfer Conf.*, pp147-152.
- Shoji, M., 1990, "Saturated Pool Boiling and Heat Transfer in High Heat Flux regime," *Pro. 2nd Typical Workshop, JSHT*, pp.66-70.
- Zhao, Y. H., Masuoka, T., and Tsuruta, T., 1997, "Theoretical Studies on Transient Pool Boiling Based on Microlayer Model (Mechanism of Transition from Nonboiling Regime to Film Boiling)," *Trans. JSME (B)*, Vol. 63, No. 607, pp.218-223.
- Zuber, N., "Hydrodynamic Aspects of Boiling Heat Transfer," AEC Report No.AECU-4439 (1959).